New Materials, Compounds and Applications
Vol.7, No.1, 2023, pp.23-36

Jomard Publishing

A NUMERICAL STUDY OF THE EFFECT OF AN OBSTACLE ON THE DISCHARGE FLOW RATE FROM A SILO IN THE CONTINUOUS REGIME

Mohamed Kechachni[1*], Mohammed Djermane[1], Mebirika Benyamine[2], Samira Laidaoui[2]

[1]Department of Civil Engineering, FIMAS laboratory, Bechar University, Algeria
[2]Department of Mechanical Engineering, FIMAS laboratory, Bechar University, Algeria

Abstract. In this paper, the discharge of a rectangular silo with a cylindrical obstacle placed just above the outlet was modeled using the discrete element method DEM. The investigation particularly focused on the flow rate and velocity distribution of particles during the discharging in a continuous regime. To provide an insight into how the obstacle may influence flow, we varied the diameter and the vertical position of the obstacle; then, we compared the results with those obtained for the discharge of a silo without an obstacle. This detailed comparison revealed several key observations. A reasonable agreement was seen between the results obtained from numerical simulations and the experimental results.

Keywords: *Granular material, discrete element method DEM, Silo, obstacle, flow rate, velocity.*

Corresponding Author: *Mohamed, Kechachni, Department of Civil Engineering, Materials and Structures Reliability Laboratory FIMAS, Bechar University, 08000, Algeria, Tel.: +213660009581, e-mail: kechachni.mohamed@univ-bechar.dz*

Received: *27 November 2022;* ***Accepted:*** *15 February 2023;* ***Published:*** *17 April 2023.*

1. Introduction

Silos are structures built to store various materials, which are important in many industrial and engineering applications (Zhao *et al.*, 2019). Depending on the ratio of outlet size and particle size, the flow can be divided into three regimes: A continuous regime, an intermittent regime, and a complete blockage of the system. The jamming occurs if the particles form an arch that spans the width of the outlet (To *et al.*, 2001; Mankoc *et al.*, 2007; 2009). It can happen when the outlet width is about 3 to 6 particle diameters (Deming & Mehring, 1929; Brown & Richards, 1958; Beverloo *et al.*, 1961; Nedderman *et al.*, 1982; Wilson *et al.*, 2014; Benyamine *et al.*, 2014). Due to operational complexities and extra energy input that other solutions require, the introduction of an obstacle to the silos provides a crucial way for some researchers to ensure the continuous and stable functioning of the discharge operation and avoid unfavorable flow phenomena (Helbing *et al.*, 2005; Zuriguel *et al.*, 2011; Alonso-Marroquin *et al.*, 2012; Lozano *et al.*, 2012; 2013; Reddy *et al.*, 2018). The effect of the insert on the properties of granular flow in silos during discharge has not been well understood, especially the discharge flow rate and velocity distribution. On reviewing the literature on this solution, the effect of inserts in silos has been studied since the

How to cite (APA):
Kechachni, M., Djermane, M., Benyamine, M., & Laidaoui S. (2023). A numerical study of the effect of an obstacle on the discharge flow rate from a silo in the continuous regime. *New Materials, Compounds and Applications, 7*(1), 23-36.

work of Johanson and Kleysteuber but mainly focused on the action and effect of the insert with different geometries on flow patterns (Johanson, 1968; Tüzün & Nedderman, 1985; Yang & Hsiau, 2001; Härtl *et al.,* 2008; Wójcik *et al.,* 2012; Zuriguel *et al.,* 2016; Murray & Alonso-Marroquin, 2016; Endo *et al.*, 2017; Katsuragi *et al.*, 2018; Sun *et al.*, 2020). However, few studies were devoted to studying the effect of obstacles on the flow rate. In the jamming regime, it has been found that the insertion of an obstacle reduces the jamming probability and induces an increase in the flow rate (Yang & Hsiau, 2001; Zuriguel *et al.*, 2011; Alonso-Marroquin *et al.*, 2012; Lozano *et al.*, 2012; 2013). Table 1 summarizes the literature according to the model, methodology, and insert type. In the continuous regime, the effect of obstacles on the discharge rate has not been thoroughly studied. In this regime, most works related to silo discharge have analyzed the influence of inserts on flow patterns (Chou & Yang, 2004; Chou *et al.*, 2006; Härtl *et al.,* 2008; Kobyłka & Molenda, 2014). For instance, Laidaoui *et al.*, 2020 experimentally studied the effect of an obstacle on the discharge flow from a rectangular silo in a continuous regime. They found that for an obstacle altitude higher than the outlet length, the obstacle had no effect on the flow rate. In contrast, when located in the zone of acceleration above the outlet, the presence of the obstacle significantly reduced the flow rate.

Table 1. Summary of the literature for the silos with inserts

References	Analysis model	Method	Insert type	Highlights
Zuriguel et al. (2011)	2D	Exp.	Disk	The pressure reduction in the area of arch formation accomplished by the obstacle is the cause of clogging reduction and hence the increase in flow rate.
Alonso-Marroquin et al. (2012)	2D	DEM Sim.	Circular	In a critical situation, the flow increases by suitably placing an obstacle.
Lozano et al. (2012)	2D	Exp.	Disk	The presence of an obstacle increases the flow rate by up to 10% compared to the silo without an obstacle.
Lozano et al. (2013)	2D	Exp.	Circular	The larger the size of the outlet, the stronger the effect of the obstacle. A decrease in discharge rate under the action of obstacle.
Yang & Hsiau (2001)	2D	DEM sim. Exp.	Conical insert BINSERT	The presence of an obstacle reduces the jamming probability and induces an increase in the flow rate.
Katsuragi et al. (2018)	2D	DEM sim. Exp.	Circular	A decrease in discharge rate in presence of inserts.
Laidaoui et al. (2020)	2D	Exp.	Cylindrical	The presence of an obstacle significantly reduces the flow, when placed in the acceleration zone above the outlet.

2. Setting up DEM simulations and validation

2.1. Description of the simulation

In this study, all simulations were carried out with a rectangular silo similar to the one used in the laboratory (Laidaoui *et al.,* 2020). Two configurations were designed, a flat bottom silo with a cylindrical obstacle of diameter D_{obs} placed at an altitude h_o and a flat bottom silo without an obstacle for comparison (Fig. 1). The dimensions of the silo and the particle properties are summarized in Table 1. The outlet size D is about 11 times greater than the grain diameter d, $D/d > 6$ ensuring the flow is in a continuous regime (Aguirre *et al.*, 2010).

Table 2. Properties of particle and silo dimensions

Parameters	Value
d (particle diameter)	$1.1\ mm$
ρ (particle density)	$2500\ kg.m^{-3}$
H (silo height)	$800\ mm$
L (silo width)	$100\ mm$
W (silo depth)	$1.5\ mm$
D (outlet size)	12.5 mm

The silo walls were assumed rigid with friction, except for the frontal walls, which were considered without friction to limit the movement of particles out of the plane.

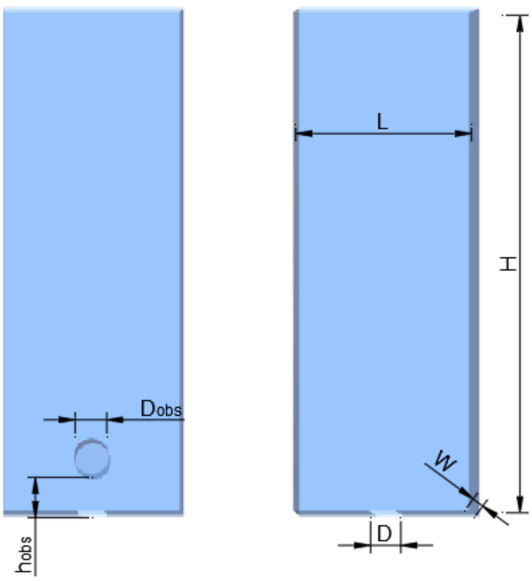

Fig. 1. Different configurations of the silo.
A flat bottom silo with a cylindrical obstacle / a flat bottom silo without an obstacle

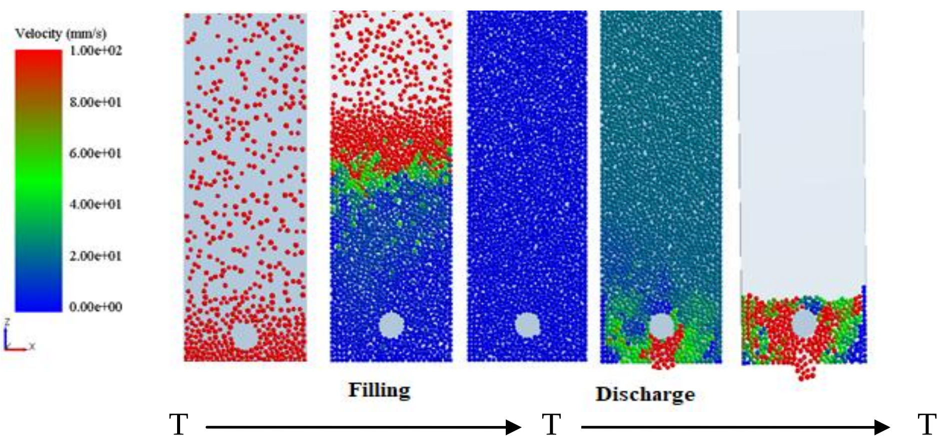

Fig. 2. The steps of the simulation process

The particles were deemed to be spheres non-cohesive in diameter $d = 1.1\ mm$, with a slight dispersion ($\pm\ 0.1\ mm$) to avoid segregation and crystallization (Pascot *et al*, 2020). The particles were randomly generated until the silo was filled at the height of $H_p = 0.72H$; when the system reached a static state, the orifice was opened, and the particles began to be discharged. Fig. 2 presents the several stages of the simulation.

A series of numerical simulations was undertaken to investigate the influence of position and obstacle diameter on the discharge flow and the velocity profiles. All possible combinations of these parameters are shown in table 3 and lead to twenty-three different configurations.

Table 3. Combinations are considered in simulations

Model	Obstacle diameter D_{obs} (mm)	Obstacle altitude h_o (mm)	Outlet length D (mm)
1	5	5	12,5
2		10	
3		15	
4		60	
5	10	5	
6		10	
7		15	
8		60	
9	20	5	
10		10	
11		15	
12		60	
13	40	5	
14		10	
15		15	
16		60	
17	No obstacle		10
18	No obstacle		12.5
19	No obstacle		15

2.2. Method and contact model

The DEM simulation approach is used to investigate the discharge flow of a silo, where the grains are treated individually and their mechanical interactions at the level of the contacts (by applying Newton's second law). This method was adapted by (Cundall & Strack, 1979) to allow the simulation of the behavior of granular media. In this study, the contact model used was based on the Hertz Mindlin no-slip contact model (Di Renzo & Di Maio, 2003), with frictional damping in the tangential direction and viscous damping in the perpendicular and tangential directions. Table 4 lists the model parameters used for the DEM simulations; these values were taken from the literature (Pascot *et al.*, 2022).

Table 4. Model parameters used in simulations.

Parameter	Value
N (number of particles)	75 000
E (Young modulus)	5×10^6 Pa
ν (Poisson coefficient)	0.22
e_{pp} / e_{pw} (restitution coefficients)	0.97 - 0.83
μ_{pp} / μ_{pw} (friction coefficients)	0.40 - 0.15

2.3. Validation

To validate the DEM model, the average mass flow was compared to the predicted flow from the empirical Beverloo equation for different outlet sizes. Beverloo proposed the most accepted law for describing the flow rate of granular materials for a flat-bottomed cylindrical hopper (Beverloo *et al*, 1961):

$$Q = C\rho\varphi_b\sqrt{g}(D - kd)^{5/2} \tag{1}$$

Where φ_b is the bulk density, g is the gravitational constant, C and k are the fitting parameters, and d and D are the diameter of the particles and the outlet length, respectively.

Many researchers modified the Beverloo correlation according to the ability to adapt to obtain a more accurate equation to express the flow rate. This correlation was generalized by (Mankoc et al., 2007, and Janda et al., 2012) in the 2D case, as follows:

$$Q = C\rho\varphi_b\sqrt{g}(D - kd)^{3/2} \tag{2}$$

For a rectangular silo at flat-bottom quasi-2D, (Benyamine *et al.*, 2017) proposed an equation derived from this law:

$$Q = C\rho\varphi_b\sqrt{g}W(D - kd)^{3/2} \tag{3}$$

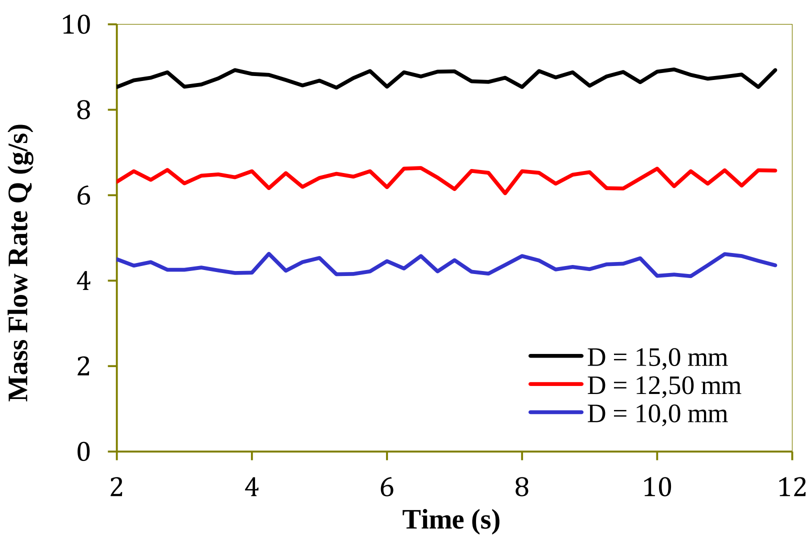

Fig. 3. Flow rate versus time for different outlet sizes

Fig. 3 shows the mass flow rate as a function of time for various outlet sizes. The discharge rate increased with the increase in the outlet size. During this time, the evolution of the flow rate obtained by the DEM model and the predicted flow rate of the Beverloo empirical equation was plotted for different outlet sizes (with $\theta = 0^o, C = 0.91$, and $k = 1.36$), (Fig. 4). The simulation results seem consistent with Beverloo prediction, which indicates that the DEM model can reasonably simulate the discharge process.

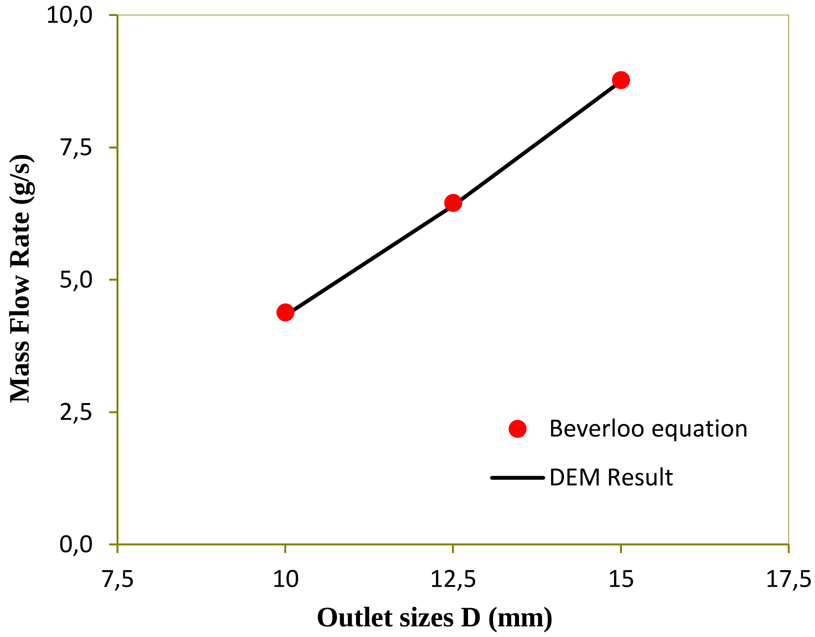

Fig. 4. Comparison of flow rates between the Beverloo Eq. [3] and the DEM simulation

3. Results and discussion

3.1. Effect of the obstacle on the discharge flow

Fig. 5 presents the plot of the temporal evolution in the mass flow rate measured during the discharge of a silo with an obstacle of diameter $D_{obs} = 40\ mm$; the obstacle is placed at different altitudes ($h_o = 5\ mm,\ h_o = 10\ mm,\ h_o = 15\ mm,\ h_o = 40\ mm,$ and $h_o = 60\ mm$, respectively). We observed that there was no difference between the simulation without an obstacle and the simulation for $h_o = 40\ mm$, and $h_o = 60\ mm$. However, the difference between simulations with no obstacle and simulations for $h_o = 5\ mm,\ h_o = 10\ mm,$ and $h_o = 15\ mm$ was more significant, as seen in Fig. 6, where the discharge mass is plotted versus time.

In Fig. 7, the mass flow rate is compared for varying obstacle altitudes and diameters for outlet size $D = 12.5mm$. The horizontal line represents the flow rate without obstacles, and the vertical lines represent the altitudes for $h_o = D$ and $h_o = 2D$, respectively.

When $h_o < D$, we can see that the flow rate is significantly reduced whenever the diameter of the obstacle is increased.

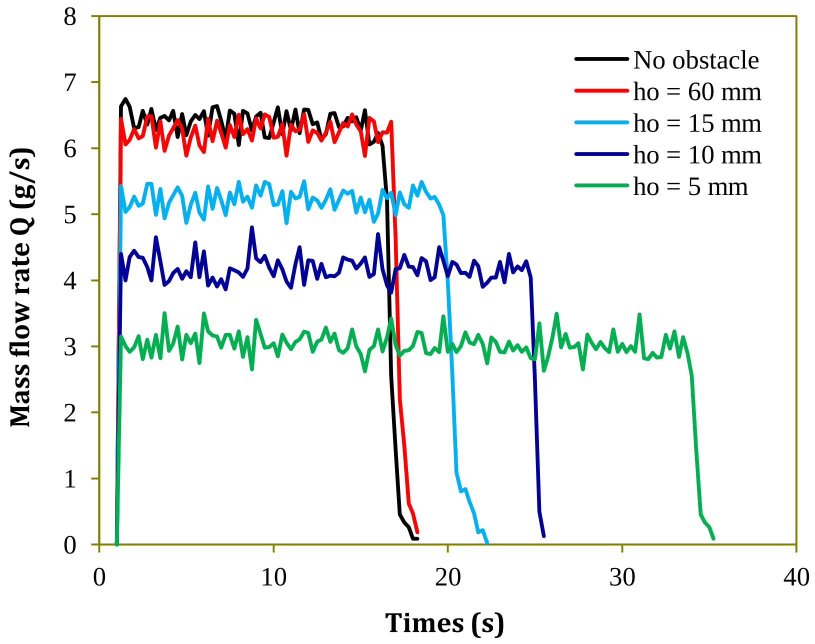

Fig. 5. Mass flow rate Q versus the time, for obstacle diameter D_{obs} $40\ mm$ and various obstacle altitude h_o

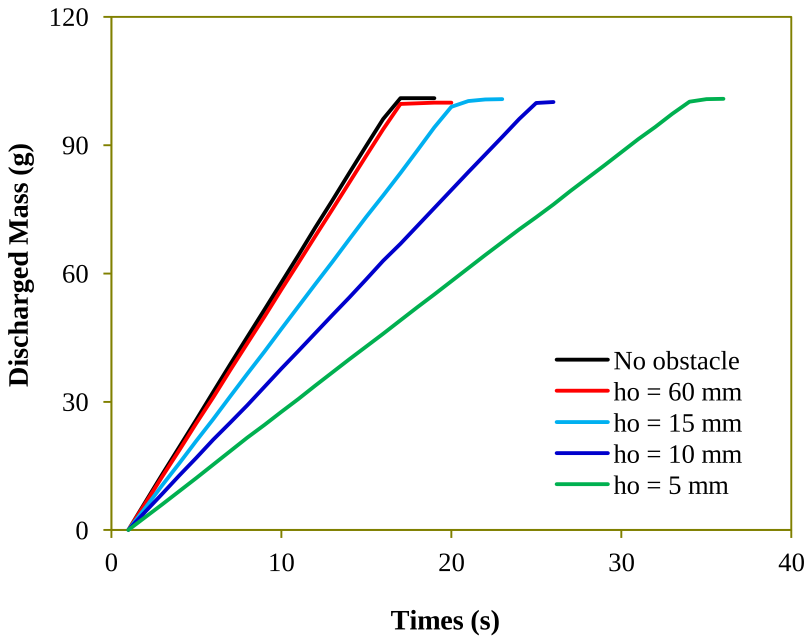

Fig. 6. Mass discharged M versus the time, for obstacle diameter D_{obs} $40\ mm$ and various obstacle altitude h_o

When $D < h_o < 2D$, the flow rate is reduced for the obstacles of diameters are bigger than D. It seems to be stabilized and reaches the value obtained with no obstacle for the obstacles of diameters smaller than D.

For $h_o > 2D$, the obstacle has no influence, and the flow rate seems to stabilize and reach the value obtained with no obstacle.

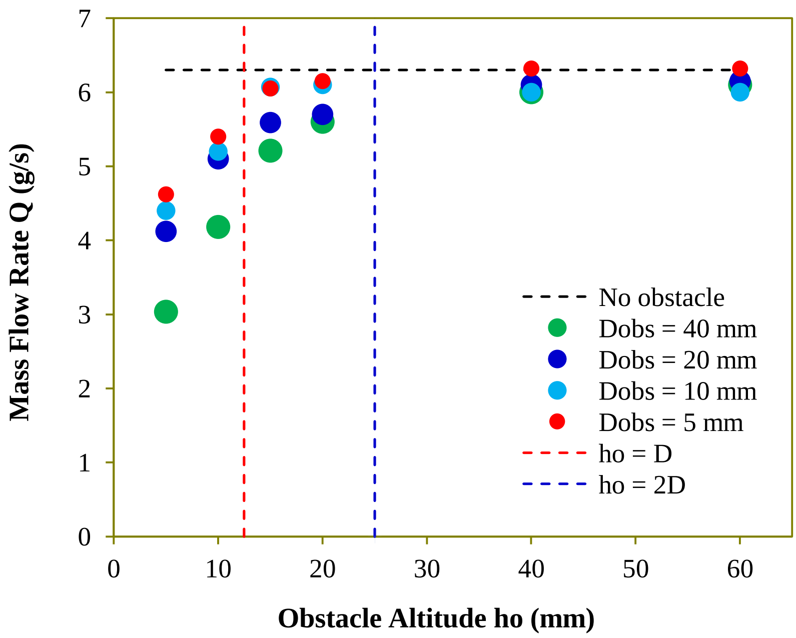

Fig.7. Mass flow rate $\boldsymbol{Q}$ versus the obstacle altitude ho for various obstacle diameters $\boldsymbol{D_{obs}}$. The horizontal line represents the flow rate without an obstacle. The vertical lines represent the altitude where $\boldsymbol{h_o = D}$ and $\boldsymbol{h_o = 2D}$, respectively

3.2. Effect of the obstacle on the velocity profiles

We compared the velocity profiles obtained during the numerical simulations for the discharge of a silo with an obstacle and those obtained for a silo without an obstacle. The velocity profiles were represented by the vertical velocity at a height $z = 5\,mm$ plotted against the position x at a moment $0.5\,s$ after discharge began. Different obstacle altitudes ($5\,mm$,$10mm$, $15\,mm$ $40\,mm$ and $60\,mm$) and obstacle diameters ($5\,mm$, $10\,mm$, $20\,mm$, and $40\,mm$) were chosen to analyze velocity profiles. In Figure 8, we present the locations and diameters of obstacles by varying this time the diameter of the obstacle D_{obs} while keeping the altitude of the obstacle h_o constant. We looked at three distinct cases:

- **a.** The case where the obstacle is placed in the area $h_o > 2D$ (Fig. 8a).
- **b.** The case where the obstacle is placed in the area $D < h_o < 2D$ (Fig. 8b).
- **c.** The case where the obstacle is placed in the area $h_o < D$ (Fig. 8c).

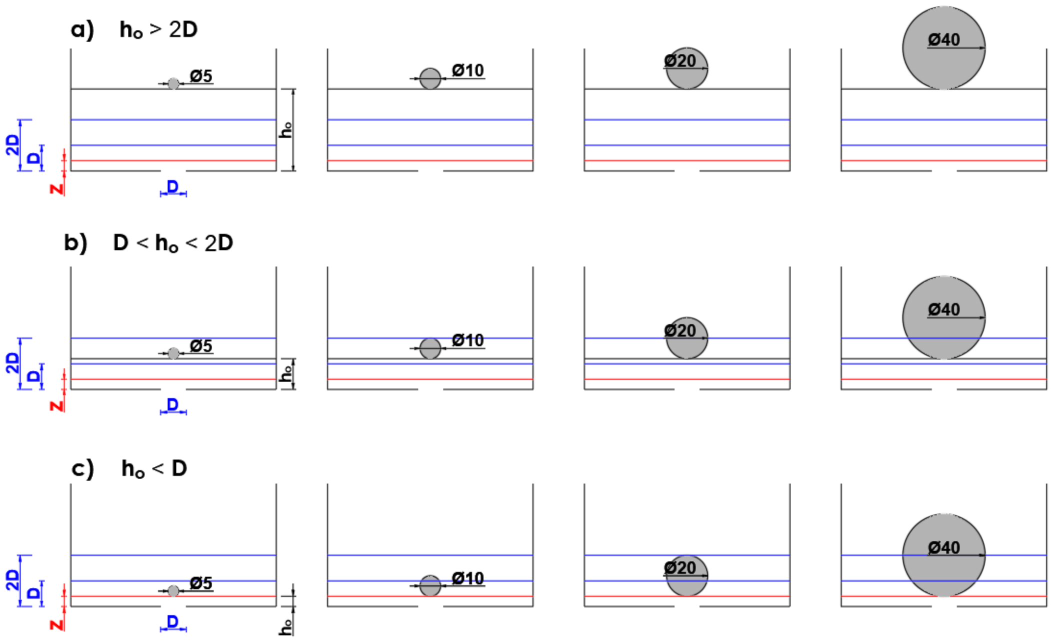

Fig. 8. Schema of different diameters of the obstacle at: the altitude $h_o > 2D$ (a), $D < h_o < 2D$ (b) and $h_o < D$ (c) in the silo model

According to the results observed in Fig. 9, it could be observed that particles having the highest velocities at the outlet ($> 600\, mm/s$) were found in the cases where the obstacle was placed at a higher altitude ($h_o > 2D$) and the cases where the obstacle had a diameter smaller than the outlet length D placed in the zone ($D < h_o < 2D$). However, low velocities ($< 400\, mm/s$) were found in cases where the obstacle was located just above the exit ($h_o < D$) and the cases where the obstacle had a diameter bigger than the outlet length D placed in the zone ($D < h_o < 2D$).

We compared the velocity profiles obtained by the simulation of a silo with an obstacle placed at different altitudes with the simulation of a silo without an obstacle. The velocity profiles are plotted in the Fig. 10, 11, and 12.

In the case where the obstacle was placed in the area $h_o < D$, the shift produced in the graphs was remarkable between the simulation without an obstacle and the simulations with an obstacle (Fig. 10). In this case, it was observed how the increase of the diameter obstacle decreased the velocity.

In the case where the obstacle was placed in the area $D < h_o < 2D$, we observed that the velocities profiles were almost unchanged and almost reached the value obtained without the obstacle for obstacle diameters smaller than the outlet length $D_{obs} < D$. When $D_{obs} > D$, we could see that the velocity was significantly reduced whenever the diameter of the obstacle was increased (Fig. 11).

In the case where the obstacle was placed in the area $h_o > 2D$, we observed that the velocities profiles were almost unchanged; whatever the diameter of the obstacle, and the velocity almost reached the value obtained without the obstacle (Fig. 12).

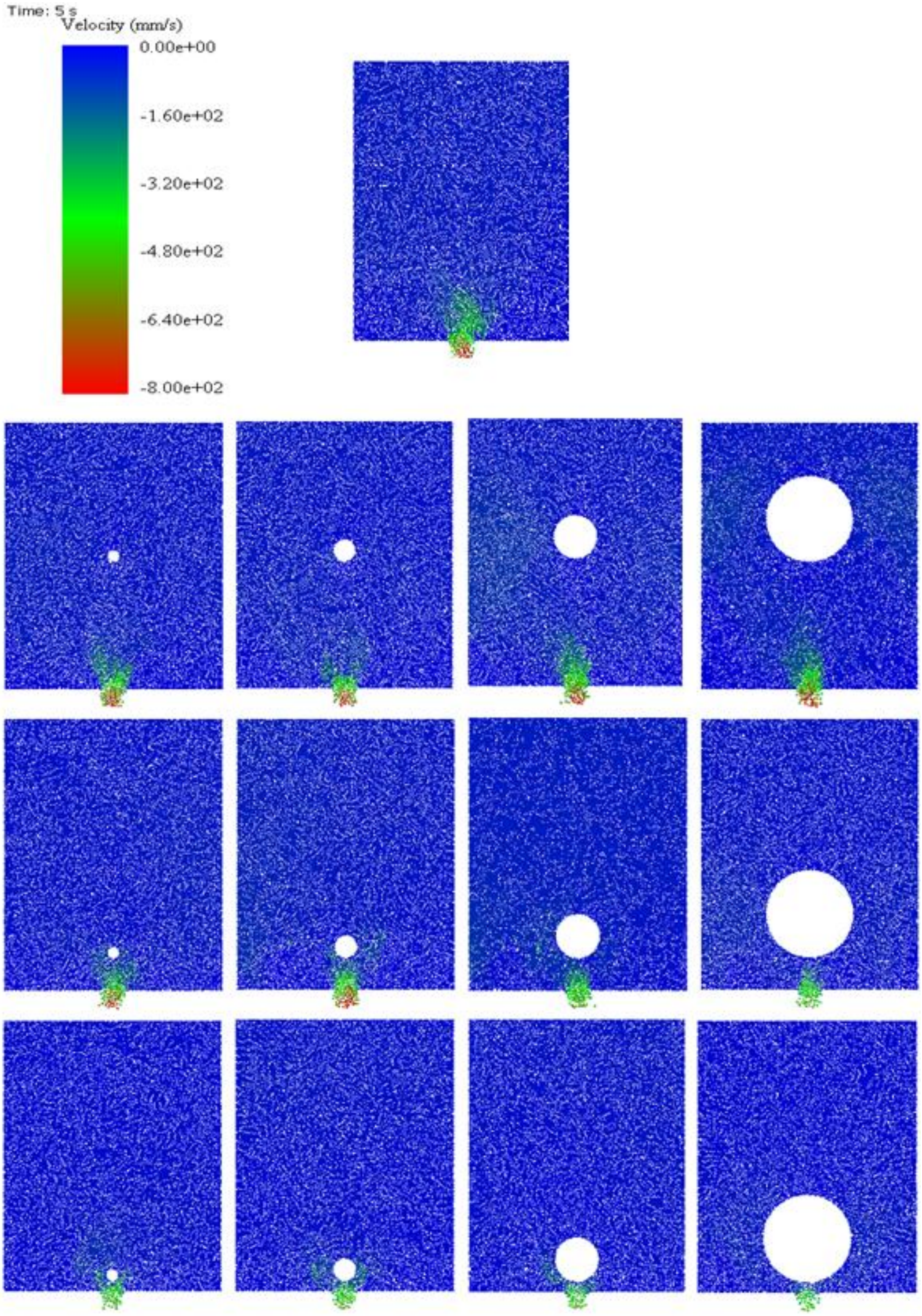

Fig. 9 A graphical representation of the velocity profiles for different obstacle diameters and altitudes, at the discharge moment 0.5 s

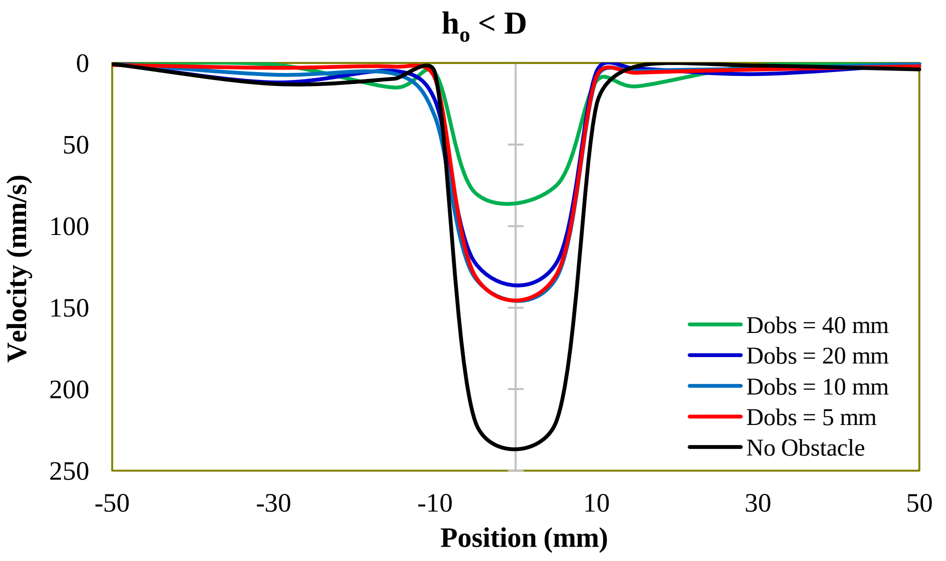

Fig. 10. Comparison of velocity profiles for a height $z = 5\ mm$ at time $t = 5\ s$ between a model without obstacle and a model with an obstacle placed at altitude $h_o < D$ and different diameter of obstacles D_{obs}

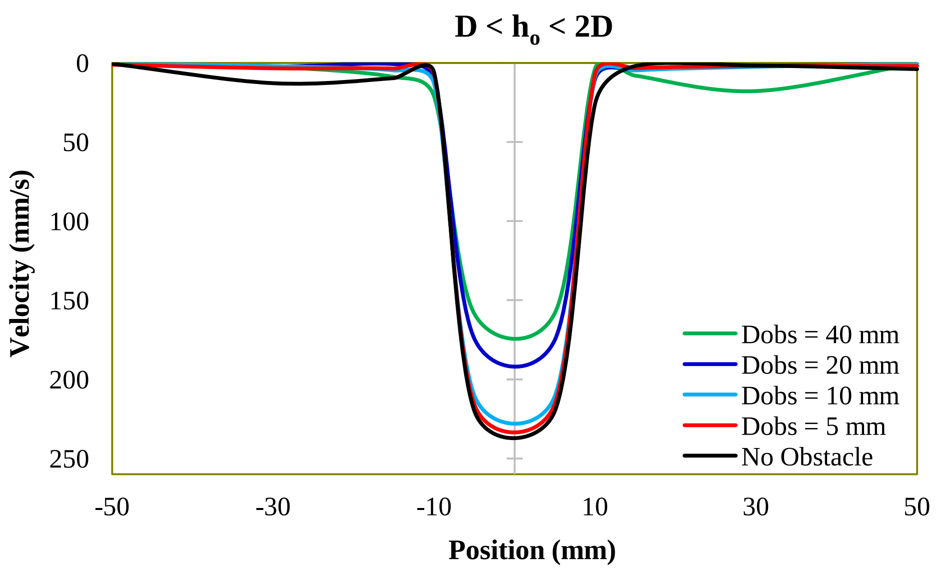

Fig. 11. Comparison of velocity profiles for a height $z = 5\ mm$ at time $t = 5\ s$ between a model without obstacle and a model with an obstacle placed at altitude $D < h_o < 2D$ and different diameter of obstacles D_{obs}

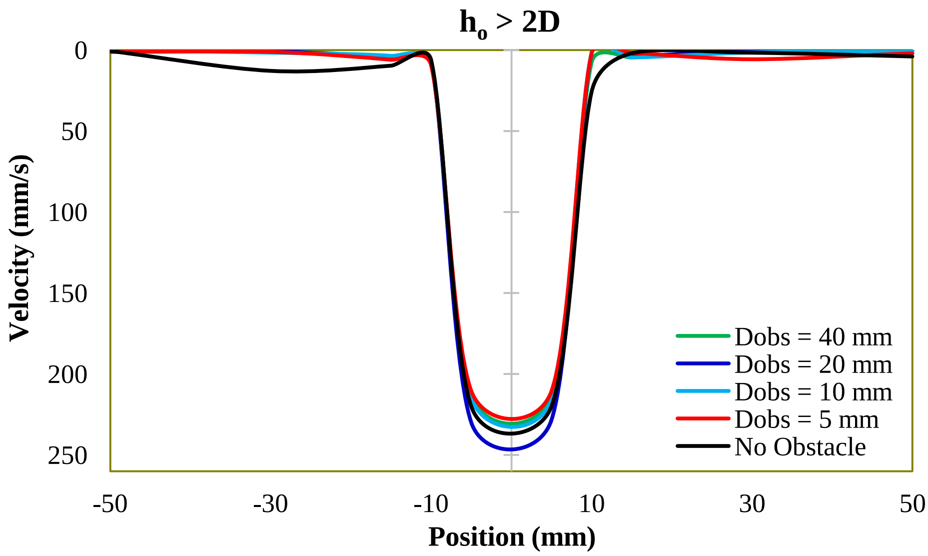

Fig. 12. Comparison of velocity profiles for a height $z = 5\ mm$ at time $t = 5\ s$ between a model without obstacle and a model with an obstacle placed at altitude $h_o > 2D$ and different diameter of obstacles D_{obs}.

4. Conclusion

This numerical study investigated the effect of a cylindrical obstacle on the flow rate during the discharge of a rectangular silo in a continuous regime using DEM.

Different locations and obstacle diameters were chosen to analyze the discharge flow rate and the velocity profiles, as well as the absence of any obstacle for comparison. The numerical results obtained were evaluated and compared with experimental results obtained by Laidaoui *et al.* 2020. The main findings could be summarized as follows:

- The analysis results obtained from the study of the velocity profiles well matched those obtained from the analysis of the discharge rate.
- For a lower obstacle placement in the silo ($h_o < D$), the obstacle had an influence, regardless of its diameter.
- For an obstacle placed in the area ($D < h_o < 2D$), the obstacle had an influence when its diameter was bigger than D.
- An obstacle placed at about two outlet lengths ($h_o > 2D$) had no influence, regardless of its diameter.
- The comparison of simulations revealed that the obstacle influenced the discharge flow rate and the velocity profiles when placed just above the orifice in the size D acceleration zone for the obstacles of diameters smaller than the outlet length D and the size $2D$ acceleration zone for the obstacles of diameters greater than D.

Reasonable agreement was seen between the results obtained from numerical simulations and the experimental results for the obstacles of diameters smaller than the outlet length D. There was a difference in the obstacles with diameters greater than D, which was probably due to the coefficient of friction of the walls or the obstacle. To better understand the physical process and the relevant parameters, future studies shall be devoted to this to this subject.

References

Aguirre, M.A., Grande, J.G., Calvo, A., Pugnaloni, L.A., & Géminard, J.C. (2010). Pressure independence of granular flow through an aperture. *Physical Review Letters*, *104*(23), 238002.

Alonso-Marroquin, F., Azeezullah, S.I., Galindo-Torres, S.A., & Olsen-Kettle, L.M. (2012). Bottlenecks in granular flow: when does an obstacle increase the flow rate in an hourglass?. *Physical Review E*, *85*(2), 020301.

Benyamine, M., Djermane, M., Dalloz-Dubrujeaud, B., & Aussillous, P. (2014). Discharge flow of a bidisperse granular media from a silo. *Physical Review E*, *90*(3), 032201.

Benyamine, M., Aussillous, P., & Dalloz-Dubrujeaud, B. (2017). Discharge flow of a granular media from a silo: effect of the packing fraction and of the hopper angle. In *EPJ Web of Conferences* (Vol. 140, p. 03043). EDP Sciences.

Beverloo, W.A., Leniger, H.A., & Van de Velde, J. (1961). The flow of granular solids through orifices. *Chemical Engineering Science*, *15*(3-4), 260-269.

Brown, R.L., Richards, J.C. (1958). Two-and Three-Dimensional flow of grains through apertures. *Nature*, *182*(4635), 600-601.

Chou, C.S., Tseng, C.Y., & Yang, T.L. (2006). Flow patterns and wall stresses in a two-dimensional bin with an obstacle. *Journal of the Chinese Institute of Engineers*, *29*(1), 1-12.

Chou, C.S., Yang, T. L. (2004). The effect of a flow corrective insert upon flow patterns and wall stresses in a two-dimensional bin-hopper. *Advanced Powder Technology*, *15*(5), 567-582.

Cundall, P.A. Strack, O.D.L. (1979). A Discrete Numerical Model for Granular Assemblies. *Géotechnique,* 29, 47.

Deming, W. E., Mehring, A. L. (1929). The gravitational flow of fertilizers and other comminuted solids. *Ind. Eng. Chem*., 21, 661.

Di Renzo, A., & Di Maio, F. P. (2004). Comparison of contact-force models for the simulation of collisions in DEM-based granular flow codes. *Chemical engineering science*, *59*(3), 525-541.

Haertl, J., Ooi, J. Y., Rotter, J. M., Wojcik, M., Ding, S. & Enstad, G.G. (2008). The influence of a cone-in-cone insert on flow pattern and wall pressure in a full-scale silo. *Chemical Engineering Research and Design*, *86*(4), 370-378.

Helbing, D., Buzna, L., Johansson, A., & Werner, T. (2005). Self-organized pedestrian crowd dynamics: Experiments, simulations, and design solutions. *Transportation Science*, *39*(1), 1-24.

Janda, A., Zuriguel, I., & Maza, D. (2012). Flow rate of particles through apertures obtained from self-similar density and velocity profiles. *Phys. Rev. Lett.*, *108* (24), 248001.

Johanson, J.R. (1966). The use of flow corrective inserts in bins *J. Eng. for Ind.,* 2, 224–230.

Johanson, J.R. (1968). The placement of inserts to correct flow in bins. *Powder Technol*., 1, 328-333.

Katsuragi, H., Anki, Reddy K., & Endo, K. (2017). Obstacle-shape effect in a two-dimensional granular silo flow field. *Phys. Rev. Fluids*, 2, 094302.

Katsuragi, H., Anki Reddy, K., & Endo, K. (2018). Shape dependence of resistance force exerted on an obstacle placed in a gravity-driven granular silo flow. *AICHE J., 64* (2018), 3849-3856.

Kobylka, R. Molenda, M. (2014). DEM simulations of loads on obstruction attached to the wall of a model grain silo and of flow disturbance around the obstruction. *Powder Technol.,* 256, 210-216.

Laidaoui, S., Aussillous, P., Djermane, M., & Dalloz-Dubrujeaud, B. (2020). Discharge flow of granular media from rectangular silos: role of an obstacle and modelling by an orifice at the corner. *Mechanics & Industry*, 21, 516.

Lozano, C., Janda, A., Garcimartín, A., Maza, D., & Zuriguel I. (2012). Flow and clogging in a silo with an obstacle above the orifice. *Phys. Rev. E*, 86, 031306.

Lozano, C., Zuriguel, I., Janda, A., Garcimartín, A., Arévalo, R., & Maza, D. (2013). Silo clogging reduction by placing an obstacle above the outlet. *AIP Conference Proceedings*.

Mankoc, C., Garcimartín, A., Zuriguel, I., Maza, D., & Pugnaloni, L. A. (2009). Role of vibrations in the jamming and unjamming of grains discharging from a silo. *Physical Review E*, *80*(1), 011309.

Mankoc, C., Janda, A., Arevalo, R., Pastor, J.M., Zuriguel, I., Garcimartín, A., & Maza, D. (2007). The flow rate of granular materials through an orifice. *arXiv preprint arXiv:0707.4550*.

Murray, A., Alonso-Marroquin, F. (2016). Increasing granular flow rate with obstructions. *Papers in Physics*, *8*(1).

Nedderman, R.M., Tüzün, U., Savage, S.B., & Houlsby, G.T. (1982). Flow of granular materials-I. Discharge rates from hoppers. *Chem. Eng. Sci.*, *37*(11).

Pascot, A., Gaudel, N., Antonyuk, S., Bianchin, J., & De Richter, S.K. (2020). Influence of mechanical vibrations on quasi-2D silo discharge of spherical particles. *Chemical Engineering Science*, 224, 115749.

Pascot, A., Morel, J.Y., Antonyuk, S., Jenny, M., Cheny, Y., & De Richter, S.K. (2022). Discharge of vibrated granular silo: A grain scale approach. *Powder Technology*, *397*, 116998.

Reddy, A.V.K., Kumar, S., Reddy, K.A., Talbot, J. (2018). Granular silo flow of inelastic dumbbells: Clogging and its reduction. *Phys. Rev. E*, 98, 022904.

Sun, D., Lu, H., Cao, J., Wu, Y., Guo, X., & Gong, X. (2020). Flow mechanisms and solid flow rate prediction of powders discharged from hoppers with an insert. *Powder Technology*, *367*, 277-284.

To, K., Lai, P.Y., & Pak, H.K. (2001). Jamming of granular flow in a two-dimensional hopper. *Physical Review Letters*, *86*(1), 71.

Tüzün, U., Nedderman, R. (1985). Gravity flow of granular materials round obstacles- I: Investigation of the effects of inserts on flow patterns inside a silo. *Chem. Eng. Sci.*, *40* (1985), 325-336.

Wilson, T.J., Pfeifer, C.R., Meysingier, N., & Durian, D.J. (2014). Granular discharge rate for submerged hoppers. *Papers in Physics*, *6*(2).

Wójcik, M., Tejchman, J., & Enstad, G.G. (2012). Confined granular flow in silos with inserts—full-scale experiments. *Powder Technol.*, 222.

Yang, S.C., Hsiau, S.S. (2001). The simulation and experimental study of granular materials discharged from a silo with the placement of inserts. *Powder Technol.*, *120* (2001), 244-255.

Zhao, Y., Yang, Y., Zhang, L., & Chew J.W (2019). Understanding the varying discharge rates of lognormal particle size distributions from a hopper using the discrete element method. *Powder Technol.*, 342.

Zuriguel, I., Janda, A., Garcimartín, A., Lozano, C., Arévalo, R., & Maza, D. (2011). Silo clogging reduction by the presence of an obstacle. *Physical Review Letters*, *107*(27), 278001.

Zuriguel, I., Olivares, J., Pastor, J.M., Martín-Gómez, C., Ferrer, L.M., Ramos, J.J., & Garcimartín, A. (2016). Effect of obstacle position in the flow of sheep through a narrow door. *Physical Review E*, *94*(3), 032302.